Molecular and electronic structures of mixed-valence exo,exo-1,12-dimethyl[1.1]ferrocenophanium triiodide

ARTICLE *in* INORGANIC CHEMISTRY · DECEMBER 1985

Impact Factor: 4.76 · DOI: 10.1021/ic00220a026

6 AUTHORS, INCLUDING:

Scott R Wilson
University of Illinois, Urbana-Champaign
389 PUBLICATIONS **11,733** CITATIONS

SEE PROFILE

Ulrich Mueller-Westerhoff
University of Connecticut
68 PUBLICATIONS **2,913** CITATIONS

SEE PROFILE

David Hendrickson
University of California, San Diego
599 PUBLICATIONS **26,739** CITATIONS

SEE PROFILE

Contribution from the School of Chemical Sciences, University of Illinois, Urbana, Illinois 61801, and Department of Chemistry, University of Connecticut, Storrs, Connecticut 06268

Molecular and Electronic Structures of Mixed-Valence *exo,exo*-1,12-Dimethyl[1.1]ferrocenophanium Triiodide

Michael F. Moore,[1] Scott R. Wilson,[1] Michelle J. Cohn,[1] Teng-Yuan Dong,[1] Ulrich T. Mueller-Westerhoff,[2] and David N. Hendrickson*[1]

Received April 22, 1985

The X-ray structure of the mixed-valence compound *exo,exo*-1,12-dimethyl[1.1]ferrocenophanium triiodide (**2**) has been determined by using direct methods, in conjunction with data measured on a four-circle diffractometer, to give discrepancy factors of R_F = 0.053 and R_{wF} = 0.045 for 2672 observed ($|F|^2 > 2.58\sigma|F|^2$) reflections. The compound crystallizes in the monoclinic space group $P2_1/c$ with four formula weights in a cell having the dimensions a = 9.458 (2) Å, b = 19.794 (6) Å, c = 13.776 (3) Å, and β = 108.23 (2)°. The calculated density is 2.182 g cm^{-3}. The two metallocene moieties in the mixed-valence cation are not equivalent. One metallocene unit has the dimensions expected for an Fe^{II} metallocene; the other is an Fe^{III} metallocene. The Fe···Fe distance in the mixed-valence cation is 4.599 (2) Å, which is close to the value reported for the unoxidized Fe^{II}_2 metallocene. The crystal packing in **2** can be described as being comprised of pairs of anions and cations that stack as units in a staggered fashion along the b axis. The I_3^- counterion is closer to the Fe^{III} ion than the Fe^{II} ion. Variable-temperature ^{57}Fe Mössbauer, magnetic susceptibility, EPR, and IR data also indicate that the mixed-valence cation is valence-localized. The triiodide salt of the dioxidized dication of *exo,exo*-1,12-dimethyl[1.1]ferrocenophane is shown to have a very weak ($|J| < \sim 0.5$ cm^{-1}) magnetic exchange interaction between the two $S = {}^1/_2$ Fe^{III} ions in the dication.

Introduction

Relatively dramatic progress has been made in the last few years toward understanding the nature of *intra*molecular electron transfer for mixed-valence biferrocenes in the *solid state*. In series **1**, all of the cations have a trans conformation in the solid state.[3-8]

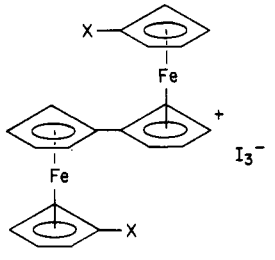

1a, X = H
b, X = I
c, X = Br
d, X = Cl
e, X = CH_2CH_3
f, X = $CH_2CH_2CH_3$

The cations in **1a**[3] and **1d**[4,5] are valence-localized from 4.2 to 300 K, as deduced by ^{57}Fe Mössbauer spectroscopy. The cations in **1b**[3,6] and **1c**[4] are valence-delocalized from 4.2 to 300 K, whereas the cations in **1e**[7] and **1f**[7,8] show a temperature dependence such that they are localized below ~200 K but become delocalized above ~290 K. The Fe···Fe distance in the cations of series **1** is ~5.1 Å. For those mixed-valence cations that are delocalized on the Mössbauer time scale, the rate of intramolecular electron transfer is in excess of $\sim 10^7$ s^{-1}. Whether or not a phase transition in the solid-state structure can occur is believed to be an explanation for the considerable variation in electron-transfer rates in the series **1a–f**.[5,9,10]

Very recently we communicated[11] the X-ray structure for the I_3^- salt of the mixed-valence *exo,exo*-1,12-dimethyl[1.1]-ferrocenophanium cation, that is, compound **2** The Fe···Fe

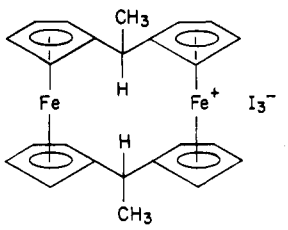

2

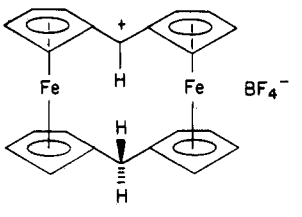

3

distance in this mixed-valence cation was found to be 4.599 (2) Å. In this paper detailed physical data are presented for compound **2** to address the question of why this mixed-valence cation is localized on the Mössbauer time scale at room temperature in spite of the relatively short Fe···Fe distance. In addition, it is interesting to compare the dimensions of the metal-oxidized mixed-valence cation in **2** with those reported[12] for the carbocation in compound **3**. Data are also presented in this paper for the dioxidized I_3^- salt of *exo,exo*-1,12-dimethyl[1.1]ferrocenophane to show that there is a very weak antiferromagnetic exchange interaction between the two $S = {}^1/_2$ ions in the Fe^{III}_2 dication.

Experimental Section

Compound Preparation. Elemental analyses were performed in the Microanalytical Laboratory of the School of Chemical Sciences.

A sample of *exo,exo*-1,12-dimethyl[1.1]ferrocenophane was prepared by the literature procedure.[13] The triiodide salt of *exo,exo*-1,12-dimethyl[1.1]ferrocenophane was prepared by dissolving 44.8 mg (0.177 mmol) of iodine in 8 mL of freshly dried and distilled CH_2Cl_2. This solution was added to a stirred solution of 50.0 mg (0.118 mmol) of *exo,exo*-1,12-dimethyl[1.1]ferrocenophane in 30 mL of dry CH_2Cl_2. The resulting green solution was stirred for 45 min. After this time a 20-mL aliquot was removed from the reaction vessel and transferred to a test tube standing in 50 mL of previously dried and distilled hexane, which was contained in a 250-mL round-bottom flask under a blanket of argon.

(1) University of Illinois.
(2) University of Connecticut.
(3) Morrison, W. H., Jr.; Hendrickson, D. N. *Inorg. Chem.* **1975**, *14*, 2331.
(4) Motoyama, I.; Suto, K.; Katada, M.; Sano, H. *Chem. Lett.* **1983**, 1215–1218.
(5) The X-ray structure of **1d** has been determined: Dong, T.-Y.; Hendrickson, D. N.; Pierpont, C. G.; Moore, M. F. *J. Am. Chem. Soc.*, in press.
(6) The X-ray structure of **1b** has been communicated: Dong, T.-Y.; Cohn, M. J.; Hendrickson, D. N.; Pierpont, C. G. *J. Am. Chem. Soc.* **1985**, *17*, 4777. The full X-ray structure is given in ref 5.
(7) Iijima, S.; Saida, R.; Motoyama, I.; Sano, H. *Bull. Chem. Soc. Jpn.* **1981**, *54*, 1375–1379.
(8) Konno, M.; Hyodo, S.; Iijima, S. *Bull. Chem. Soc. Jpn.* **1982**, *55*, 2327–2335.
(9) Dong, T.-Y.; Hendrickson, D. N.; Iwai, K.; Cohn, M. J.; Geib, S. J.; Rheingold, A. L.; Sano, H.; Motoyama, I.; Nakashima, S. *J. Am. Chem. Soc.*, in press.
(10) Hendrickson, D. N.; Oh, S. M.; Dong, T.-Y.; Kambara, T.; Cohn, M. J.; Moore, M. F. *Comments Inorg. Chem.*, in press.
(11) Moore, M. F.; Wilson, S. R.; Hendrickson, D. N.; Mueller-Westerhoff, U. T. *Inorg. Chem.* **1984**, *23*, 2918–2920.
(12) Mueller-Westerhoff, U. T.; Nazzal, A.; Prössdorf, W.; Mayerle, J. J.; Collins, R. L. *Angew. Chem., Int. Ed. Engl.* **1982**, *21*, 293–294.
(13) Cassens, A.; Eilbracht, P.; Nazzal, A.; Prössdorf, W.; Mueller-Westerhoff, U. T. *J. Am. Chem. Soc.* **1981**, *103*, 6367–6372.

0020-1669/85/1324-4559$01.50/0

Table I. Experimental and Crystal Data for the X-ray Structure of *exo,exo*-1,12-Dimethyl[1.1]ferrocenophanium Triiodide (**2**)

Crystal Parameters	
cryst syst: monoclinic	space group: $P2_1/c$
a = 9.458 (2) Å	α = 90°
b = 19.794 (6) Å	β = 108.23 (2)°
c = 13.776 (3) Å	γ = 90°
V = 2449.6 (10) Å^3	Z = 4
fw = 804.86	μ = 49.37 cm^{-1}
ρ(calcd) = 2.182 g cm^{-3}	
faces: {100}, {10$\bar{2}$}, {010}	

Data Measurement
radiation: graphite-monochromatized Mo Kα (λ = 0.710 69 Å)
2θ limits: 3.0° < 2θ < 55.0°
scan range: −0.8° to +1.0°
data measd: 6294
data used ($\|F\|^2 > 2.58\sigma\|F\|^2$): 2672
transmissn factor limits: 0.271 to 0.553
internal consistency: R_i = 0.019; $R_F{}^a$ = 0.053; $R_{wF}{}^a$ = 0.045

$^a R_F = \sum||F_o| - |F_c||/\sum F_o$; $R_{wF} = [\sum w(F_o - |F_c|)^2/\sum wF_o^2]^{1/2}$.

Slow evaporation of the solvent led to the formation of large green crystals that were suitable for X-ray diffraction. The remainder of the reaction solution was stirred rapidly while 2 mL of hexane was slowly added. The green crystals that were seen to precipitate immediately were filtered and washed with hexane. Anal. Calcd for $C_{24}H_{24}Fe_2I_3$: C, 35.81; H, 3.01; Fe, 13.88; I, 47.30. Found: C, 35.75; H, 3.12; Fe, 13.77; I, 46.87.

The dioxidized salt of *exo,exo*-1,12-dimethyl[1.1]ferrocenophane was prepared by first dissolving 50.0 mg (0.118 mmol) of the parent ferrocene in 30 mL of freshly dried and distilled CH_2Cl_2. A 40-mL saturated solution of I_2 dissolved in CH_2Cl_2 was added slowly dropwise via a dropping funnel to the solution of *exo,exo*-1,12-dimethyl[1.1]-ferrocenophane. The resulting dark green crystals were filtered and washed repeatedly with CH_2Cl_2. Anal. Calcd for $C_{24}H_{24}Fe_2I_8$: C, 20.03; H, 1.68; Fe, 7.76; I, 70.53. Found: C, 20.70; H, 1.42; Fe, 7.62; I, 70.61.

Physical Methods. Variable-temperature (5.8–300 K) magnetic susceptibilities were measured with a SQUID magnetometer. Corrections for background and sample diamagnetism were made.

Iron-57 Mössbauer spectra were collected with a constant-acceleration spectrometer, which has been described.[14] Least-squares fitting of the powdered-sample Mössbauer spectra with Lorentzian lines was carried out by using a modified version of a previously reported computer program.[15] It should be noted that the isomer shifts illustrated in the figures are plotted as experimentally obtained.

X-Band EPR spectra of powdered samples were collected on a Bruker ER200 X-band spectrometer employing an Oxford Instruments temperature controller. A calibrated copper–constantan thermocouple was used to determine sample temperatures.

Infrared spectra were obtained with a Nicolet Model MX-5 spectrometer. All samples were prepared as 13-mm KBr pellets with 2–5 mg of compound mixed well with 150 mg of KBr.

Electronic absorption spectra were measured at room temperature with a Varian Model 2300 spectrophotometer.

Crystal Measurements and Structure Determination. The opaque, green prismatic crystal used for data collection was roughly equidimensional with well-defined faces, edges, and corners (0.14 × 0.22 × 0.28 mm). Preliminary precession photography showed that the crystal symmetry is monoclinic and that the measured density and unit cell volume are consistent with the proposed molecular formula.

The crystal was mounted onto a Syntex $P2_1$ automated four-circle diffractometer. Crystal data are given in Table I. The intensities of 6294 reflections were measured at 298 K with the 2θ–θ-scan technique employing graphite-monochromated Mo Kα radiation and a scan speed variable from 2.0 to 19.5°/min. Corrections were made for Lorentz and polarization effects, as well as for absorption.

The structure was solved by direct methods.[16] Correct positions for the 3 iodine atoms were deduced from an E map. The first weighted difference Fourier summation gave positions for the iron atoms, and a second summation using calculated structure factors based on all 5 atoms revealed the remaining 24 non-hydrogen atomic positions. Following several cycles of least-squares refinement, only a few hydrogen atoms surfaced in the difference Fourier map; consequently, the hydrogen positions were calculated. In the final cycle of least squares, all non-hydrogen atoms were refined with anisotropic thermal coefficients and a group isotropic thermal parameter was refined for the hydrogen atoms that were fixed in "idealized" positions. Successful convergence was indicated by the maximum change/error for the last cycle, 0.05; there were no high correlations.

The final atomic positional parameters are given in Table II.

Table II. Positional Parameters for *exo,exo*-1,12-Dimethyl[1.1]ferrocenophanium Triiodide (**2**)[a]

	x/a	y/b	z/c
I(1)	0.2747 (1)	0.10006 (4)	0.16257 (7)
I(2)	0.60001 (9)	0.10618 (3)	0.22197 (6)
I(3)	0.9226 (1)	0.10728 (5)	0.27794 (7)
Fe(1)	0.3947 (2)	0.34013 (7)	0.0923 (1)
Fe(2)	0.8400 (2)	0.34128 (8)	0.3526 (1)
C(1)	0.388 (1)	0.3746 (5)	0.2317 (7)
C(2)	0.325 (1)	0.3087 (6)	0.2134 (8)
C(3)	0.240 (1)	0.3121 (7)	0.1195 (9)
C(4)	0.190 (1)	0.3794 (7)	0.0825 (9)
C(5)	0.305 (1)	0.4177 (5)	0.1531 (9)
C(6)	0.508 (1)	0.4017 (5)	0.3265 (7)
C(7)	0.632 (1)	0.3546 (5)	0.3780 (7)
C(8)	0.758 (1)	0.3769 (6)	0.4665 (8)
C(9)	0.849 (1)	0.3216 (7)	0.5019 (8)
C(10)	0.791 (1)	0.2650 (6)	0.4381 (8)
C(11)	0.659 (1)	0.2862 (5)	0.3640 (7)
C(12)	0.428 (1)	0.4245 (5)	0.4038 (8)
C(13)	0.594 (1)	0.3566 (5)	0.0681 (8)
C(14)	0.478 (1)	0.3754 (6)	−0.0185 (8)
C(15)	0.384 (1)	0.3185 (7)	−0.0546 (9)
C(16)	0.446 (1)	0.2644 (6)	0.0101 (10)
C(17)	0.578 (1)	0.2861 (6)	0.0865 (8)
C(18)	0.718 (1)	0.4065 (7)	0.1250 (8)
C(19)	0.842 (1)	0.3795 (6)	0.2110 (8)
C(20)	0.909 (1)	0.3138 (7)	0.2291 (10)
C(21)	1.036 (2)	0.3171 (9)	0.320 (1)
C(22)	1.039 (2)	0.382 (1)	0.357 (1)
C(23)	0.929 (1)	0.4224 (7)	0.2934 (9)
C(24)	0.788 (2)	0.4384 (8)	0.052 (1)
H(2)	0.3564	0.2700	0.2553
H(3)	0.1424	0.2752	0.0875
H(4)	0.1186	0.3959	0.0223
H(5)	0.3225	0.4646	0.1480
H(6)	0.5562	0.4374	0.3031
H(8)	0.7735	0.4213	0.4941
H(9)	0.9366	0.3214	0.5595
H(10)	0.8328	0.2210	0.4445
H(11)	0.5978	0.2581	0.3118
H(121)	0.3492	0.4546	0.3710
H(122)	0.4970	0.4468	0.4598
H(123)	0.3887	0.3861	0.4278
H(14)	0.4636	0.4191	−0.0484
H(15)	0.2955	0.3175	−0.1117
H(16)	0.4055	0.2200	0.0041
H(17)	0.6429	0.2593	0.1390
H(18)	0.6656	0.4375	0.1537
H(20)	0.8761	0.2748	0.1881
H(21)	1.1040	0.2817	0.3483
H(22)	1.1092	0.3978	0.4189
H(23)	0.9131	0.4692	0.3019
H(241)	0.7124	0.4566	−0.0046
H(242)	0.8420	0.4050	0.0292
H(243)	0.8535	0.4735	0.0859

[a] Estimated standard deviations for last significant figure are given in parentheses.

Results and Discussion

Molecular Structure of *exo,exo*-1,12-Dimethyl[1.1]-ferrocenophanium Triiodide (2). A stereoview of the mixed-valence cation in compound **2** is shown in Figure 1. Interatomic distances and bond angles are collected in Table III. The two metallocene moieties in the cation are not equivalent. As found before for the mixed-valence diferrocenylselenium monocation $(I_3^-{\cdot}I_2{\cdot}^1/_2CH_2Cl_2$

(14) Cohn, M. J.; Timken, M. D.; Hendrickson, D. N. *J. Am. Chem. Soc.* **1984**, *106*, 6683–6689.
(15) Chrisman, B. L.; Tumolillo, T. A. *Comput. Phys. Commun.* **1971**, *2*, 322.
(16) Main, P.; Fiske, S. J.; Hull, S. E.; Lessinger, L.; Germain, G.; Declercq, J.-P.; Woolfson, M. M., MULTAN 80, a system of computer programs for the automatic solution of crystal structures from X-ray diffraction data.

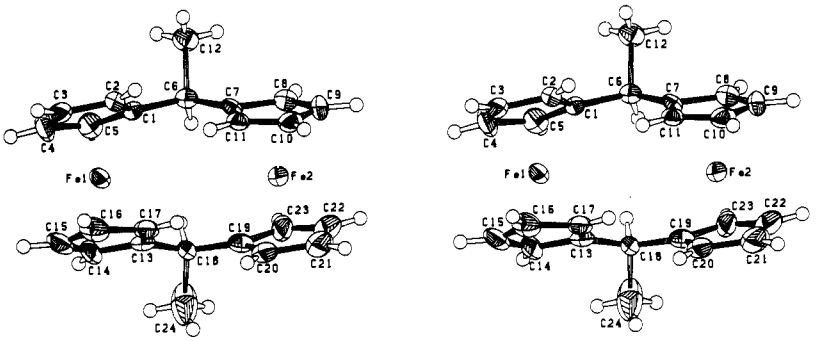

Figure 1. ORTEP stereoview of the mixed-valence *exo,exo*-1,12-dimethyl[1.1]ferrocenophane cation in compound **2** with 35% probability ellipsoids.

salt),[17] the centroid-to-centroid distance [3.31 (2) Å] between the two rings associated with atom Fe(1) indicates that this metallocene unit is in the Fe^{II} oxidation state. The centroid-to-centroid distance [3.39 (2) Å] associated with Fe(2) indicates that this is the Fe^{III} metallocene moiety.

The Fe···Fe distance in the mixed-valence monocation of compound **2** is 4.599 (2) Å. This value is intermediate between the values seen for the two crystallographically distinct molecules of the neutral unoxidized complex.[19] The Fe···Fe distances found for the two crystallographically different molecules in the unoxidized complex are 4.595 (2) and 4.620 (2) Å. Clearly, there is little movement of the two iron ions in this mixed-valence cation, as had been observed[18] for the mixed-valence bis(fulvalene)diiron cation, where the Fe···Fe distance is 0.35 Å shorter in the mixed-valence cation than in unoxidized bis(fulvalene)diiron.

Information about the conformational relationship between the two iron metallocene units in a mixed-valence molecule is critical to a detailed understanding of the rate of thermal electron transfer. As can be seen in Figure 1, the two metallocene moieties are twisted relative to each other. This is to be expected for two such units joined by sp^3-hybridized carbon centers. The dihedral angle between ring 1 (C(1)–C(5)) and ring 2 (C(7)–C(11)) is 28.0°. Similarly, the observed angle between ring 3 (C(13)–C(17)) and ring 4 (C(19)–C(23)) is 28.9°.

For both bridging carbon atoms there exists a significant difference in the displacement of the atom from the planes of the two cyclopentadienyl rings to which it is attached. Carbon bridging atom C(6) deviates from the best plane through ring 1 by 0.159 (9) Å, whereas it lies 0.076 (9) Å out of the plane of ring 2. For carbon bridging atom C(18) the corresponding deviations are 0.02 (1) and 0.10 (1) Å. Rings 1 and 3 associated with Fe(1) are not quite parallel, with the angle between them being 5.2°. The dihedral angle between rings 2 and 4 is 4.8°. Hence, the monocation of **2** can be described as being comprised of two metallocene moieties with a dihedral angle between them of roughly 28°. There are two crystallographically independent molecules in the unit cell of unoxidized *exo,exo*-1,12-dimethyl-[1.1]ferrocenophane.[19] The dihedral angles between the metallocene units of these two molecules are 30.1 and 31.3°.

The average bond length and bond angle for the bridging carbon atoms C(6) and C(18) are 1.52 (2) Å and 111.2 (9)°, respectively. These values are in good agreement with observations from the unoxidized complex[19] and strongly indicate sp^3 hybridization for these bridging carbon atoms.

As can be clearly seen in Figure 1, the cation in **2** adopts the exo-methyl configuration as was found[19] in the crystal structure of the unoxidized complex. [1.1]Ferrocenophanes are flexible and, if the substituents allow, can interconvert between two syn-oriented conformations. In *exo,exo*-1,12-dimethyl[1.1]ferrocenophane this would amount to a conversion of the exo,exo form to the sterically impossible endo,endo analogue. The structure confirms that only the exo,exo-oriented isomer exists.

Table III. Interatomic Dimensions for *exo,exo*-1,12-Dimethyl[1.1]ferrocenophanium Triiodide[a]

	Distances (Å)		
C(1)–C(2)	1.42 (1)	C(7)–C(8)	1.48 (1)
C(2)–C(3)	1.44 (2)	C(8)–C(9)	1.39 (2)
C(3)–C(4)	1.42 (2)	C(9)–C(10)	1.42 (2)
C(4)–C(5)	1.43 (2)	C(10)–C(11)	1.40 (1)
C(5)–C(1)	1.41 (1)	C(11)–C(7)	1.40 (1)
C(13)–C(14)	1.40 (2)	C(19)–C(20)	1.43 (2)
C(14)–C(15)	1.42 (2)	C(20)–C(21)	1.43 (2)
C(15)–C(16)	1.40 (2)	C(21)–C(22)	1.39 (3)
C(16)–C(17)	1.43 (2)	C(22)–C(23)	1.38 (2)
C(17)–C(13)	1.43 (2)	C(23)–C(19)	1.45 (2)
Fe(1)–C(1)	2.058 (10)	Fe(2)–C(7)	2.122 (10)
Fe(1)–C(2)	2.07 (1)	Fe(2)–C(8)	2.08 (1)
Fe(1)–C(3)	2.03 (1)	Fe(2)–C(9)	2.07 (1)
Fe(1)–C(4)	2.05 (1)	Fe(2)–C(10)	2.06 (1)
Fe(1)–C(5)	2.06 (1)	Fe(2)–C(11)	2.07 (1)
Fe(1)–C(13)	2.04 (1)	Fe(2)–C(19)	2.10 (1)
Fe(1)–C(14)	2.04 (1)	Fe(2)–C(20)	2.08 (1)
Fe(1)–C(15)	2.04 (1)	Fe(2)–C(21)	2.10 (2)
Fe(1)–C(16)	2.03 (1)	Fe(2)–C(22)	2.04 (2)
Fe(1)–C(17)	2.06 (1)	Fe(2)–C(23)	2.09 (1)
C(6)–C(1)	1.53 (1)	C(18)–C(13)	1.55 (2)
C(6)–C(7)	1.49 (1)	C(18)–C(19)	1.48 (2)
C(6)–C(12)	1.55 (1)	C(18)–C(24)	1.50 (2)
Fe(1)–Fe(2)	4.599 (2)		
centroid 1–centroid 2	3.31 (2)	centroid 3–centroid 4	3.39 (2)
I(1)–I(2)	2.929 (1)	I(2)–I(3)	2.903 (1)
	Angles (deg)		
C(1)–C(2)–C(3)	106.9 (10)	C(7)–C(8)–C(9)	107.9 (10)
C(2)–C(3)–C(4)	109 (1)	C(8)–C(9)–C(10)	108.9 (10)
C(3)–C(4)–C(5)	106.9 (10)	C(9)–C(10)–C(11)	107.4 (10)
C(4)–C(5)–C(1)	108.9 (9)	C(10)–C(11)–C(7)	110.4 (9)
C(5)–C(1)–C(2)	108.4 (9)	C(11)–C(7)–C(8)	105.3 (9)
C(13)–C(14)–C(15)	109 (1)	C(19)–C(20)–C(21)	108 (1)
C(14)–C(15)–C(16)	107 (1)	C(20)–C(21)–C(22)	106 (1)
C(15)–C(16)–C(17)	110 (1)	C(21)–C(22)–C(23)	112 (1)
C(16)–C(17)–C(13)	106.2 (9)	C(22)–C(23)–C(19)	107 (1)
C(17)–C(13)–C(14)	108.1 (10)	C(23)–C(19)–C(20)	106 (1)
C(1)–C(6)–C(7)	116.7 (8)	C(13)–C(18)–C(19)	117 (1)
C(1)–C(6)–C(12)	107.2 (8)	C(13)–C(18)–C(24)	110.6 (9)
C(7)–C(6)–C(12)	109.5 (8)	C(19)–C(18)–C(24)	106.5 (10)
I(1)–I(2)–I(3)	177.90 (4)		

[a] Hydrogen atoms were fixed in idealized positions, 0.95 Å from the carbon atoms to which they are attached.

A comparison of the structure of the mixed-valence cation in **2** with the structure reported[12] for the carbenium monocation in **3** is interesting. The dihedral angle between the two metallocene moieties in the mixed-valence cation in **2** is greater than that found for the carbocation of **3**. The four distances between the two iron atoms in the mixed-valence cation of **2** and the bridging carbon atoms C(6) and C(18) are all about equal (3.3 Å). On the other hand, the apparently positively charged carbon atom in **3** is noticeably drawn toward the center of the cation, lying approximately 0.20 Å below the intersection of the two adjacent cyclopentadienyl ring planes [Fe···C^+ distances of 2.96 (2) and 3.01 (2) Å]. The

(17) Kramer, J. A.; Herbstein, F. H.; Hendrickson, D. N. *J. Am. Chem. Soc.* **1980**, *102*, 2293–2301.
(18) Hillman, M.; Kvick, A. *Organometallics* **1983**, *2*, 1780.
(19) (a) McKechnie, J. S.; Bersted, B.; Paul, I. C.; Watts, W. E. *J. Organomet. Chem.* **1967**, *8*, 29. (b) McKechnie, J. S.; Maier, C. A.; Bersted, B.; Paul, I. C. *J. Chem. Soc., Perkin Trans. 2* **1973**, 138.

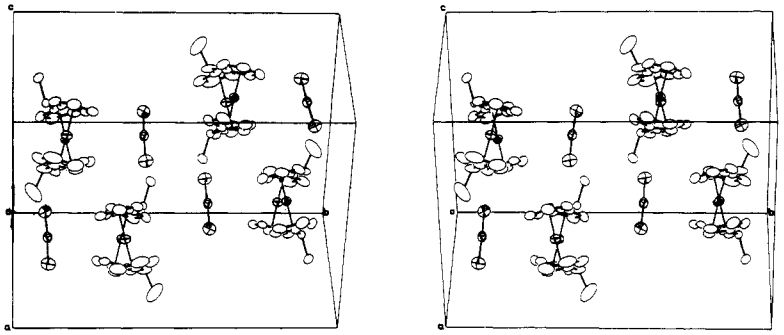

Figure 2. Stereo packing diagram of *exo,exo*-1,12-dimethyl[1.1]ferrocenophanium triiodide (**2**) viewed along the Fe(1)–Fe(2) vector.

"positive" carbon atom in **3** moves to interact with the two iron centers. This same type of distortion to establish an interaction between positively charged carbon atom and iron atom was also seen in **4**.[20] The two ring carbon–bridging carbon bond distances

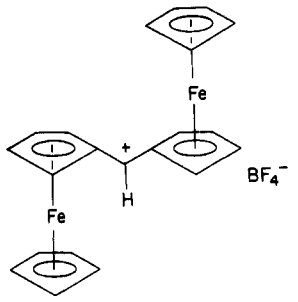

4

in **4** were found to be 1.42 and 1.39 Å, indicating a different orbital hybridization. These distances are considerably shorter than those observed for compound **2**.

The triiodide anion in **2** is essentially linear and lies roughly parallel to the *a* axis. The I(1)–I(2)–I(3) angle is 177.90 (4)° and is comparable to the value of 177.17 (5)° observed in the triiodide salt of diferrocenyl selenium.[17] There is asymmetry associated with the bond lengths found in the triiodide anion. The distance from I(1) to I(2) is 2.929 (1) Å, while the distance from I(2) to I(3) is 2.903 (1) Å.

Crystal-Packing Arrangement in 2. As will be seen in future papers,[5,9,10,21,22] in order to understand what controls the rate of intramolecular electron transfer for mixed-valence complexes *in the solid state*, it will be necessary to examine the details of the packing arrangement in the solid state. If the anion is not placed symmetrically relative to the two metal sites in a mixed-valence cation, this can affect the rate of *intra*molecular electron transfer. Furthermore, it appears[9,10] that if the anion can become *dynamically* disordered at high temperatures such that on the average it is disposed symmetrically relative to the two metal sites in a mixed-valence cation, this will also dramatically influence the rate of electron transfer within the cation.

The crystal packing in **2** can be described as being comprised of pairs of anions and cations that stack as units in a staggered fashion along the *b* axis. A stereoview of the crystal packing is shown in Figure 2. In this stereoview the unit cell is oriented such that the viewing direction is approximately parallel to the Fe···Fe vectors in the cations.

A plane may be positioned so as to contain both Fe(1) and Fe(2) and pass through the centers of mass of all four cyclopentadienyl rings as closely as possible. The normal distances from this plane to the iodine atoms of the nearest I_3^- anion are 4.7088 (8), 4.6375 (6), and 4.6654 (10) Å, respectively, for atoms I(1), I(2), and I(3). Two vectors may be constructed to describe further the relationship between the cation and the nearest I_3^- anion. One vector is drawn from Fe(1) to Fe(2). The second vector is constructed along all three iodine atoms in the I_3^- anion. The angle between these two vectors is 32.78°. This relative positioning of cation and nearest I_3^- anion is evident in Figure 2. It seems likely that the positioning of the I_3^- anion in **2** influences the valence localization for this mixed-valence cation. The possibility that ion pairs exist in the solid state with the I_3^- anion more closely associating with the Fe^{III} half of the mixed-valence cation is intriguing.

Presumably due to the exo,exo-dimethyl configuration of the molecule, the triiodide anion in **2** approaches the side of the cation opposite the methyl groups. As is clearly illustrated in Figure 2, the cation has hydrogen atoms on ring carbons C(11) and C(17) that are directed in such a way that the central iodine atom of the triiodide anion develops relatively close contacts. The contact distances from I(2) to H(11) and H(17) are 3.26 (6) and 3.31 (7) Å, respectively. It could be a combination of these weak C–H···I bonds and the electrostatic attraction of the anion for the more positive iron ion that leads to the asymmetric placement of the I_3^- anion relative to the cation. The distances from Fe(1) to I(1), I(2), and I(3) are 5.049 (2), 5.122 (2), and 6.687 (2) Å, respectively. The distances from Fe(2) to those same three atoms are 7.034 (2), 5.243 (2), and 4.860 (2) Å, respectively. One of the negative charge-carrying terminal atoms of the I_3^- anion is closer to Fe(2) than is the other I_3^- terminal atom to Fe(1). This asymmetric placement of the I_3^- anion relative to the cation should influence the rate of electron transfer in the cation.

The positioning of the I_3^- anion relative to the mixed-valence cation in **1f** apparently is also important. This compound gives a Mössbauer spectrum at temperatures below ~200 K that exhibits both Fe^{II} and Fe^{III} doublets.[7] As the temperature of **1f** is increased above ~200 K, the two doublets move together to become a single average valence doublet at temperatures greater than 245 K. The X-ray structure of **1f** has been reported[8] at 110 and 298 K. At 110 K **1f** crystallizes in space group $P\bar{1}$; the cation in **1f** at 110 K is asymmetric with Fe^{II} and Fe^{III} halves. Without going into detail, it is interesting to note that the I_3^- anion is positioned closer to the Fe^{III} ion at this temperature. The shortest Fe^{III}···I distance is 4.93 (1) Å at 110 K. At 298 K **1f** crystallizes in space group $P\bar{1}$ and both the mixed-valence cation and the I_3^- anion are sitting on centers of symmetry. Thus, at 298 K the I_3^- anion is symmetrically disposed relative to the two iron ions in the cation of **1f**. Furthermore, C–H···I contacts between the cation and anion in the range of 3.24 (7)–3.37 (14) Å were noted in the 110 K structure.

The temperature dependence of the rate of *intra*molecular electron transfer in **1f** likely involves a change from a static positioning of the I_3^- anion at low temperature to a dynamic motion of the anion at higher temperatures. The apparent centrosymmetric nature of the I_3^- anion at 298 K results from an average of the two positions that the I_3^- anion is moving between. If the structural work on **1f** does give an accurate view of changes in the structure from 110 to 298 K, then it seems very likely that there is a phase transition present. The existence of a phase transition involving order–disorder in **1f** should be substantiated by some type of thermal analysis such as differential thermal

(20) Cais, M.; Dani, S.; Herbstein, F. H.; Kapon, M. *J. Am. Chem. Soc.* **1978**, *100*, 5554–5558.
(21) Oh, S. M.; Hendrickson, D. N.; Hassett, K. L.; Davis, R. E. *J. Am. Chem. Soc.* **1984**, *106*, 7984–7985.
(22) (a) Oh, S. M.; Hendrickson, D. N.; Hassett, K. L.; Davis, R. E. *J. Am. Chem. Soc.*, in press. (b) Sorai, M.; Kaji, K.; Hendrickson, D. N.; Oh, S. M. *J. Am. Chem. Soc.*, in press.

Table IV. ^{57}Fe Mössbauer Fitting Parameters for *exo,exo*-1,12-Dimethyl[1.1]ferrocenophane and Related Systems[a]

compd	T, K	ΔE_Q	δ[b]	Γ[c]	
2	280	2.374 (4)	0.364 (2)	0.258 (6)	0.248 (6)
		0.185 (14)	0.354 (7)	0.478 (25)	0.372 (16)
	238	2.386 (2)	0.376 (1)	0.242 (3)	0.256 (4)
		0.210 (7)	0.349 (4)	0.512 (13)	0.348 (7)
	178	2.396 (3)	0.390 (1)	0.258 (4)	0.262 (4)
		0.248 (27)	0.350 (14)	0.712 (27)	0.444 (12)
	123	2.404 (2)	0.402 (1)	0.254 (2)	0.264 (2)
		0.248 (27)	0.350 (14)	1.704 (56)	0.586 (10)
4[d]		2.10	0.435		
3[e]		1.80	0.436		
5	300	0.174 (20)	0.381 (10)	0.490 (41)	0.346 (20)
	250	0.182 (15)	0.399 (8)	0.488 (37)	0.356 (16)
	200	0.185 (14)	0.393 (7)	0.576 (34)	0.334 (11)
	140	0.189 (17)	0.393 (8)	0.682 (43)	0.386 (12)
ferrocenium triiodide	300	0.156 (24)	0.417 (12)	0.646 (62)	0.338 (16)
	180	0.218 (17)	0.436 (9)	0.844 (52)	0.378 (10)
	120	0.245 (37)	0.442 (18)	1.422 (146)	0.508 (16)

[a] ΔE_Q and δ values are given in units of mm/s; the estimated standard deviations in the least significant figures are given in parentheses. [b] Isomer shift relative to iron metal at room temperature. [c] Full width at half-height taken from the least-squares fitting program. The width for the line at more negative velocity is listed first for each doublet. [d] Gleiter, R.; Seeger, R.; Binder, H.; Fluck, E.; Cais, M. *Angew. Chem., Int. Ed. Engl.* **1972**, *11*, 1028. [e] Data given in supplementary material for ref 12.

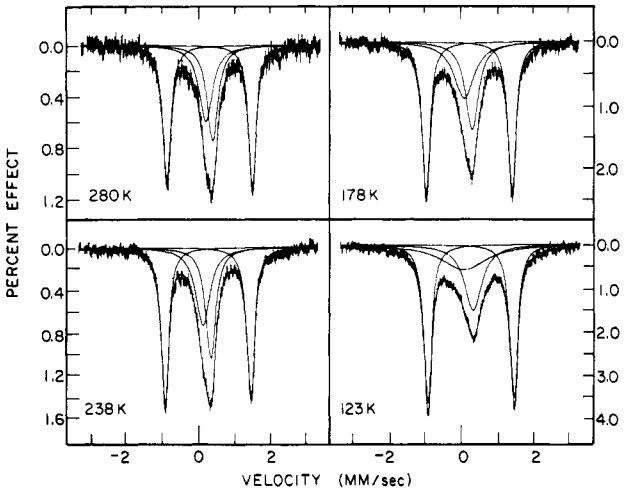

Figure 3. ^{57}Fe Mössbauer spectra of *exo,exo*-1,12-dimethyl[1.1]-ferrocenophanium triiodide (2) at various temperatures. The velocity scale is referenced to iron metal.

analysis, differential scanning calorimetry, or heat capacity determination.

Physical Properties of 2. In the previous ^{57}Fe Mössbauer work[3,23] on the mixed-valence compound **2**, it was suggested that both the valence-localized and the valence-delocalized forms of the cation in **2** are present in the solid state. That is, more than two doublets were seen in the spectrum at many temperatures. This is not in agreement with the single-crystal X-ray structure reported in this paper. As a consequence, a new sample of **2** was examined with Mössbauer spectroscopy. Figure 3 illustrates the spectra obtained at four different temperatures. The absorption peaks in each spectrum were least-squares fit to Lorentzian lines, and the resulting fitting parameters are summarized in Table IV, together with data for related complexes.

The Mössbauer spectra in Figure 3 look similar to those reported[3,23] previously, except the third quadrupole-split doublet with a splitting of ~1.9 mm/s is *not* seen. In the previous report, the spectral area associated with this third doublet was found to be relatively small. In the case of this new sample of **2**, the Mössbauer spectra exhibit only Fe^{II} (outer doublet) and Fe^{III} (inner doublet) signals at each temperature. Furthermore, as can be seen in Figure 3, good fits of the spectra are possible at all temperatures when the areas of the Fe^{II} and Fe^{III} doublets are constrained to be equal.

(23) Morrison, W. H., Jr.; Hendrickson, D. N. *Chem. Phys. Lett.* **1973**, *22*, 119–123.

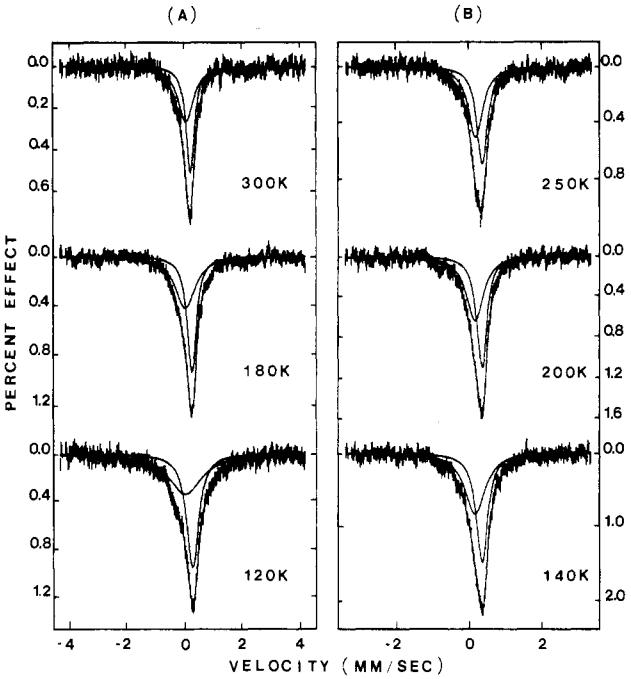

Figure 4. ^{57}Fe Mössbauer spectra for ferrocenium triiodide (A) and compound **5** (B). The velocity scale is referencd to iron metal.

Several additional new samples of **2** were prepared under different reaction conditions as well as under the conditions employed previously.[3,23] In no case was a third doublet seen in the Mössbauer spectrum. At this time it is *not* clear what the origin of the third doublet is. Perhaps some amount of the carbocation from *exo,exo*-1,12-dimethyl[1.1]ferrocenophane (i.e., analogue of **3**) was formed in the previous preparations of **2**. A more probable possibility is that the previous samples of 1,12-dimethyl[1.1]ferrocenophane contained both exo,exo and exo,endo isomers.

Closer examination of the Mössbauer spectra illustrated in Figure 3 for **2** shows that particular care has to be exercised in order to properly fit the Fe^{III} signal. In fact, at first it appears that the ratio of the Fe^{III} to Fe^{II} signal is decreasing as the temperature of **2** is decreased. A careful analysis shows, however, that the Fe^{III} signal should be fit by two equal-area Lorentzian lines at each temperature. The asymmetry of the Fe^{III} doublet increases as the temperature is decreased. This same type of fitting is found for the Mössbauer spectra of ferrocenium triiodide (see Figure 4). Two Lorentzian lines with quite different line widths

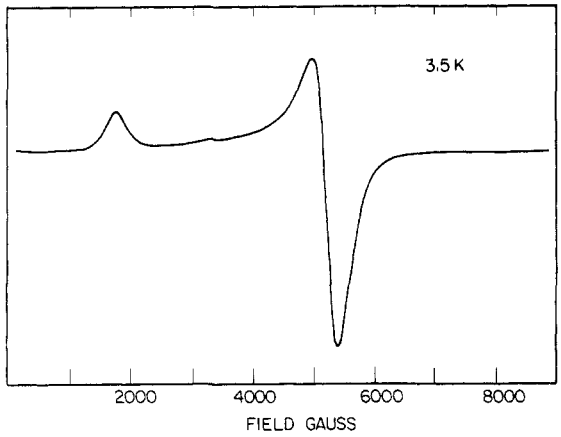

Figure 5. X-Band EPR spectrum of a powdered sample of *exo,exo*-1,12-dimethyl[1.1]ferrocenophanium triiodide at 3.5 K.

are employed at each temperature. Quite possibly slow paramagnetic relaxation effects are operational here. The suggested negative value of the EFG is in agreement with findings for other ferrocenium cations.[14,24] Additional substantiation for the validity of this fitting is found in plotting the logarithm of the total Mössbauer spectral area vs. absolute temperature. If there is no change in the vibrational nature of a solid across the given temperature range, the Debye model of a solid would lead to a straight line for a plot of ln (area) vs. temperature. Linear plots of ln (area) vs. temperature were obtained both from the above analysis of the ferrocenium triiodide Mössbauer spectra and from the above analysis of the total spectral area in the Mössbauer spectra of **2** (figure available in supplementary material).

A 3.5 K X-band EPR spectrum was run for a polycrystalline sample of **2** (see Figure 5). The appreciable **g**-tensor anisotropy observed in this spectrum is consistent with what is found for localized mixed-valence biferrocenes and for monomeric ferrocenium species. The two principal features present in the spectrum are characterized by $g_\perp = 1.32$ and $g_\parallel = 3.87$. Biferrocenium triiodide (**1a**) has g values of 1.72 and 3.58 at 12 K in the solid state.[3] Prior to the present study this was the largest **g**-tensor anisotropy reported for a mixed-valence biferrocene. These large **g**-tensor anisotropies reflect the fact that the single unpaired electron is localized on one iron ion; the resulting electronic state has considerable orbital angular momentum. Ferrocenium triiodide has an even more anisotropic **g** tensor with $g_\perp = 1.26$ and $g_\parallel = 4.35$.[25]

Variable-temperature magnetic susceptibility data were obtained for **2** from 250 to 20 K (figure available in supplementary material). The effective magnetic moment per Fe^{III} ion (i.e., per formula weight of **2**) varies from 2.63 μ_B at 250 K to 2.54 μ_B at 20 K. These results are consistent with the appreciable **g**-tensor anisotropy found in the EPR experiment.

Infrared spectroscopy has also been employed to study valence localization in mixed-valence ferrocenes.[26] The perpendicular cyclopentadienyl C–H bending mode for a Fe^{II} metallocene typically occurs in a range from 805 to 815 cm^{-1}. The corresponding band for an Fe^{III} metallocene is found in the range from 840 to 850 cm^{-1}. The KBr-pellet IR spectra of **2** and unoxidized *exo,exo*-1,12-dimethyl[1.1]ferrocenophane are compared in Figure 6. The IR data for these two compounds are given in the supplementary material. The unoxidized compound has a C–H bending mode at 810 cm^{-1}. Compound **2** shows two strong bands in this region, one at 816 cm^{-1} and the other at 843 cm^{-1}. The IR spectrum for mixed-valence **2** is thus seen to exhibit two C–H bending bands, which may be readily assigned to Fe^{II} and Fe^{III} moieties. It is clear that **2** is localized on the IR time scale.

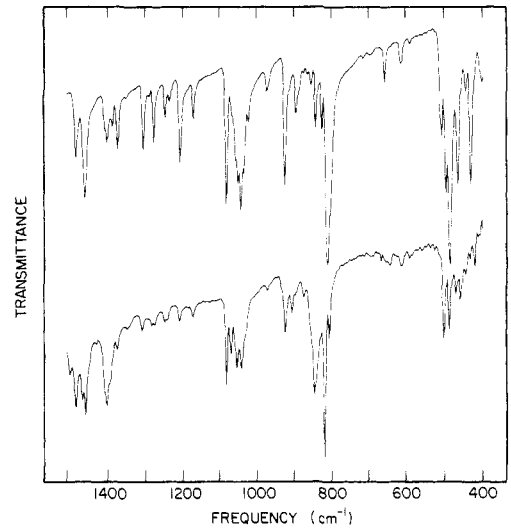

Figure 6. Infrared spectra of room-temperature KBr pellets of *exo,exo*-1,12-dimethyl[1.1]ferrocenophane (top) and the mixed-valence compound **2** (lower).

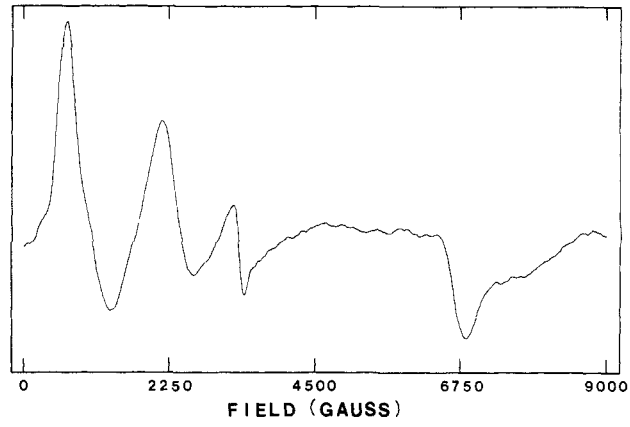

Figure 7. X-Band EPR spectrum of a powdered sample of dioxidized compound **5** at 3.3 K.

Triiodide Salt of Dioxidized *exo,exo*-1,12-Dimethyl[1.1]-ferrocenophane. When a large excess of I_2 is used as an oxidant, the dark green crystalline compound **5** is isolated. The dication

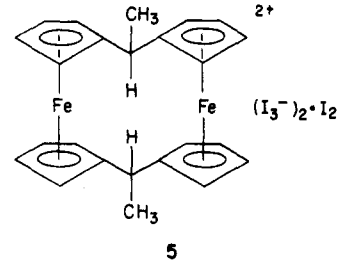

5

in this compound has two Fe^{III} ions, each of which possesses one unpaired electron. The Fe^{III} composition of **5** is verified by the Mössbauer spectra of **5**, which are shown in Figure 4. Least-squares fitting parameters are given in Table IV. Each spectrum is fit to two Lorentzian lines. The small quadrupole splittings of 0.189 (17) mm/s at 140 K and 0.174 (20) mm/s at 300 K are very similar to the values found for ferrocenium triiodide. A plot of ln (area) vs. temperature for the Mössbauer data of **5** gives a straight line.

X-Band EPR spectra were run at 3.3, 33, and 60 K for a ground polycrystalline sample of **5**. The 3.3 K spectrum is shown in Figure 7. This spectrum is seen to be composed of four signals. At higher temperatures these four signals become broader and eventually disappear into the background at temperatures above ~60 K. It is clear that the 3.3 K spectrum shown in Figure 7 is *not* characteristic of either a mononuclear Fe^{III} metallocene or a va-

(24) Morrison, W. H., Jr.; Hendrickson, D. N. *Inorg. Chem.* **1974**, *13*, 2279–2280.
(25) (a) Anderson, S. E.; Rai, R. *Chem. Phys.* **1973**, *2*, 216. (b) Duggan, D. M.; Hendrickson, D. N. *Inorg. Chem.* **1975**, 14, 955.
(26) Kramer, J. A.; Hendrickson, D. N. *Inorg. Chem.* **1980**, *19*, 3330.

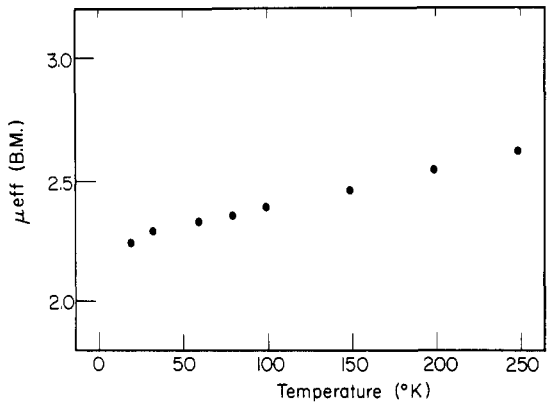

Figure 8. Plot of effective magnetic moment per iron ion (μ_{eff}) vs. temperature for dioxidized compound **5**.

lence-localized mixed-valence biferrocene. The two $S = {}^1/_2$ Fe^{III} ions in the dication of **5** must be involved in a magnetic exchange interaction that gives $S = 0$ and $S = 1$ states for the binuclear dication. The EPR signal arises from complexes that are in the $S = 1$ state. Two $\Delta M_s = \pm 1$ EPR transitions would be observed for each of the two principal components of the **g** tensor. Thus, the $g_\perp$ and $g_\parallel$ signals seen for an Fe^{III} ion (such as seen in Figure 5) each would be split into two signals by zero-field splitting. The zero-field splitting could result from either a through-space interaction of the two magnetic dipoles, one located at each Fe^{III} ion, or a pseudodipolar interaction. In the latter case, the $S = 1$ state is split by a spin-orbit interaction with an excited state. It is unfortunately not an easy matter to analyze the spectrum shown in Figure 7 for two reasons. First, since the spectrum encompasses such a large magnetic field range, including a portion of it very near zero field, it is difficult to simulate by the eigenfield method. Second, as seen for **2**, the two Fe^{III} metallocene moieties in **5** would be expected to be twisted relative to each other. The **g** tensors at the two Fe^{III} ions would most likely be misaligned. Single-crystal EPR data would be needed to interpret the EPR spectrum of **5**.

Magnetic susceptibility data were collected for **5** from 250 to 5.8 K. Figure 8 shows a plot of μ_{eff} per iron atom vs. temperature. As can be seen, μ_{eff}/Fe varies from 2.67 to 2.20 μ_B. There is no sign of an appreciable magnetic exchange interaction between the two $S = {}^1/_2$ ions in the dication of **5**. This is interesting since the Fe···Fe distance is ~4.6 Å and the unpaired-electron-containing $d_{x^2-y^2}/d_{xy}$ orbitals at each iron ion are directed from one iron toward the other iron ion. The exchange interaction that is indicated by the EPR results must be of such a magnitude that $|J|$ is less than ~0.5 cm^{-1}, where J is the exchange parameter in the spin Hamiltonian $\hat{H} = -2J\hat{S}_1 \cdot \hat{S}_2$.

An IR spectrum for a KBr pellet of **5** is available in the supplementary material. It is important to note that there is a strong C-H bending band at 847 cm^{-1}. This is a value that is appropriate for an Fe^{III} metallocene.

Conclusions and Comments

The X-ray structure of **2** indicates a valence-localized structure for the mixed-valence *exo,exo*-1,12-dimethyl[1.1]ferrocenophane cation. Mössbauer, EPR, magnetic susceptibility, and IR data are in agreement with the structural results.

The dioxidized compound **5** has two $S = {}^1/_2$ Fe^{III} ions that are involved in a very weak intramolecular magnetic exchange interaction where the exchange parameter $|J|$ is less than ~0.5 cm^{-1}. It is curious that the $DDQH^-$ (monoanion of hydroquinone of 2,3-dicyano-5,6-dichloro-*p*-benzoquinone) salt of the dication in **5** has previously been reported[3] to possess a strong antiferromagnetic exchange interaction. It is possible that the dication in the $DDQH^-$ salt was the carbocation where both of the positive charges reside on the two bridging carbon atoms.

Acknowledgment. We are grateful for support from National Institutes of Health Grant HL13652 (D.N.H.).

Supplementary Material Available: Tables V-VII, listing structure factors and thermal parameters for compound **2** and IR data for *exo,exo*-1,12-dimethyl[1.1]ferrocenophane and for compounds **2** and **5**, and Figures 9-11, including plots of ln (area) of Mössbauer spectra vs. temperature for **2**, **5**, and ferrocenium triiodide, a plot of μ_{eff} vs. temperature for **2**, and a 400-1500-cm^{-1} IR spectrum of a KBr pellet of **5** (17 pages). Ordering information is given on any current masthead page.

Contribution from the Department of Chemistry, Purdue University, West Lafayette, Indiana 47907

Use of Spin-Magnetization-Transfer Techniques To Probe the Dynamic Behavior of (Dialkylamido)dimolybdenum Complexes

Timothy W. Coffindaffer, William M. Westler, and Ian P. Rothwell*

Received February 15, 1985

Addition of 2,6-diphenylphenol (HOAr) to the dinuclear compound $Mo_2(NMe_2)_6$ results in the formation of 1,2-$Mo_2(OAr)_2(NMe_2)_4$ when hexane is used as the solvent and 1,1,2-$Mo_2(OAr)_3(NMe_2)_3$ when benzene is used as the solvent. Solution spectra are consistent with the presence of the gauche rotamer for 1,2-$Mo_2(OAr)_2(NMe_2)_4$, showing two types of NMe_2 groups, and the unique atom bond to each metal gauche to one another for 1,1,2-$Mo_2(OAr)_3(NMe_2)_3$, showing three types of NMe_2 groups. Variable-temperature ^1H NMR studies allow the activation energy for restricted rotation about the M-NMe_2 bonds to be estimated from coalescence temperatures while the use of spin-magnetization-transfer techniques has allowed more accurate measurements of the activation parameters for this process. Two-dimensional NMR has also been applied to probe possible rotation in these molecules about the Mo≡Mo bond.

Introduction

One of the most powerful uses of nuclear magnetic resonance spectroscopy is its application to the study of dynamic chemical processes.[1] In inorganic and organometallic chemistry this technique has allowed a number of exchange processes to be characterized that would otherwise not be amenable to study by other techniques. In particular, stereochemical nonrigidity and ligand fluxionality are important areas where it is possible to obtain relatively accurate kinetic measurements and such measurements have had an important impact on other aspects of chemistry in particular bonding ideas.

A series of molecules that exhibit a diverse and rich range of dynamic processes are early-transition-metal dinuclear complexes.[2] Here, dimer-monomer equilibria, bridge-terminal ligand exchange and, restricted (both electronic and steric) ligand mobility have been characterized in a number of systems.[3] Of particular interest

(1) Jackman, L. M.; Cotton, F. A. "Dynamic Nuclear Magnetic Resonance Spectroscopy"; Academic Press: New York, 1975.

(2) Cotton, F. A.; Walton, R. A. "Multiple Bonds Between Metal Atoms"; Wiley: New York, 1982.

0020-1669/85/1324-4565$01.50/0